Plasma Chemistry and Plasma Processing (2024) 44:393–410
https://doi.org/10.1007/s11090-023-10379-y

ORIGINAL PAPER

Biological and Chemical Reactivities of Plasma-Activated Water Prepared at Different Temperatures

Zhenyu Zhou[1] · Haiyu Li[1] · Zhihua Qi[2] · Dongping Liu[1]

Received: 20 April 2023 / Accepted: 9 August 2023 / Published online: 22 August 2023
© The Author(s), under exclusive licence to Springer Science+Business Media, LLC, part of Springer Nature 2023

Abstract
In this study, plasma activated water (PAW) has been prepared by using atmospheric pressure air dielectric barrier discharge (DBD) at the PAW temperature of 3–90 °C. The effects of PAW temperature, pH values and O_3 concentration on the *E. coli* inactivation have been studied, and the chemical reactivity of PAW has been analyzed by using the chemical probe. It is found that both the biological and chemical reactivities of PAW are strongly dependent on the PAW temperature, however, their dependences on temperature are not consistent. When the PAW temperature decreases from 90 to 3 °C, the chemical reactivity of PAW is significantly increased due to an increase in the concentration of activated oxygen in PAW. Decreasing the temperature from 30 to 3 °C or increasing the temperature from 45 to 90 °C leads to an obvious increase in the biological reactivity of PAW. Our analysis shows that an obvious increase in the biological reactivity of low-temperature ($\leq$15 °C) PAW is due to the synergistic effect of acidic solutions and a high concentration of activated oxygen in PAW. The high biological reactivity of PAW at the temperature of $\geq$60 °C can be attributed to the synergistic effect of acidic solutions, heat and the activated oxygen, such as O_3 and HOONO.

Keywords Plasma activated water · Plasma inactivation · Atmospheric pressure air plasma · Chemical reactivity · Biological reactivity · Temperature

Introduction

Plasma-activated water (PAW) is usually produced during the direct or indirect interactions between the atmospheric pressure air plasmas and the water to be treated [1, 2], which simulate the generation of reactive oxygen and nitrogen species (RONS) in the lighting and their subsequent dissolution into rainwater, rivers, lakes or seas. During these interactions, the discharge energy is stored into PAW, and the PAW containing various RONS is chemically unstable. Thus, PAW is a natural product reacting with the living things on the planet. PAW has been used for decreasing the viability of cancer (NOS2) cells [3], inactivation of

✉ Dongping Liu
dpliu@dlut.edu.cn

[1] School of Electrical Engineering, Dalian University of Technology, Dalian 116024, China

[2] Basic Teaching Department, Shenyang Institute of Engineering, Shenyang 110136, China

S. aureus on strawberry [4], promoting the seed germination and seeding growth [5], inhibiting SARS-CoV-2 infection [6], wound healing [7], and nitrogen fixation [8].

PAW contains short-lived (S-lived) and long-lived (L-lived) RONS. The main components of S-lived RONS with their lifetimes of < 1–2 ms include hydroxyl radicals (OH), singlet oxygen (O_2 ($^1\Delta_g$)), superoxide anions (O_2^-) and water anions (H_2O^-), nitric oxide radicals (NO, NO_2) while L-lived RONS include hydrogen peroxide (H_2O_2), peroxynitrite (HOONO), ozone (O_3), nitrate (HNO_3), and nitrite (HNO_2). The HOONO lifetime is about 1 s at the room temperature, and they can convert into HNO_3 [9]. The S-lived RONS in the aqueous solution are mainly produced during the interaction between air plasma and water, resulting in their solution. The S-lived RONS in the aqueous solution tend to convert into L-lived RONS, accompanied by the release of chemical energy. L-lived RONS can be generated due to the dissolution of L-lived RONS in the gas phase or the chemical reactions related to S-lived RONS in water. It has been widely accepted that the HOONO in the aqueous solution can decompose into S-lived RONS, such as OH and NO_2, which plays a crucial role in controlling the chemical reactivity of PAW. HOONO can be generated via the H_2O_2 reaction with HNO_2 in the acidic PAW, as shown below.

$$H^+ + H_2O_2 + HNO_2 \rightarrow HOONO + H_2O + H^+ \quad (1)$$

Both H_2O_2 and HNO_2 are L-lived RONS, thus HOONO can be one of the most important RONS in PAW.

Very complex chemical reactions occurred in PAW, which are thus affected by the PAW temperature. The study by Tsoukou et al. [10] indicated that the concentrations of chemical species in PAW were affected by the storage at different temperatures. The PAW became very stable when stored at the temperature of ≤ -80 °C, and it achieved 6 log reduction of *S. aureus and E. coli* after 18 months. Arda et al. found that maintaining PAW at low temperatures was not an adequate recourse to preserve the reactive species [11]. However, the conservation of reactive species and restoration of bactericidal activity of PAW was achieved via low-temperature storage and pH adjustment. To address the limitations of the short lifetime of the RONS in PAW, plasma-activated hydrogels were developed by Chen et al. to act as reactive species carriers that allow good storage and controlled slow-release of RONS to preserve its antimicrobial reactivity for more than 14 days [12]. The study by Shen J et al. [13] showed that PAW stored at -80 °C retained bactericidal activity, and attributed to the fact that low temperatures contribute to the maintenance of H_2O_2 and NO_2^- concentrations. Similarly, PAW prepared from the DBD source used in the study by Subramanian G et al. [14] retained a large proportion of its potency against cancer cells after 14 days of refrigerated storage at − 20 °C. Rathore et al. [15] found that storing PAW at 4 °C for two weeks resulted in small changes in physicochemical properties, NO_3^- and H_2O_2 concentrations, but significantly decreases in NO_2^- and O_3. And the study showed the interaction of the stirrer speed and temperature had a significant effect on the ORP of PAW. Pang B et al. [16] demonstrated that the chemical activity of activated water prepared using the plasma jet was higher at 25 °C than at 40 °C, 70 °C and 4 °C, which was related to the high surface tension at 25 °C.

This study by Choi et al. evaluated the effect of a sequential combination of washing treatments using PAW and mild heating at 60 °C on the inactivation of background microbiota and inoculated foodborne pathogens of shredded salted Chinese cabbages [17]. The treatment with PAW led to 2.0, 2.2, 1.8, and 0.9 log CFU/g reduction in mesophilic aerobic bacteria, lactic acid bacteria, yeast, moulds and coliforms, respectively. The subsequent mild heating treatment decreased the counts of lactic acid bacteria, yeast and moulds below

the detection limit. The synergistic effect of PAW and mild heat on the inactivation of *S. cerevisiae* on grapes was evaluated by Xiang et al. [18]. The maximum inactivation efficiency of *S. cerevisiae* cells was 5.85 Log CFU/g after the PAW treatment at 55 °C for 30 min, which was much higher than that of PAW treatment at 25 °C (2.39 Log CFU/g). After the mild heat at 25–55 °C for 30 min, the concentrations of H_2O_2 and NO_2^- in PAW significantly decreased, accompanied by an increase in NO_3^- content. It was suggested that the synergistic effect of PAW and mild heat increased the membrane permeability, which contributed to the leakage of intracellular components, such as nucleic acids and proteins [19]. In the study by Tian Y et al. [20], temperatures of 31.5 °C and 38.1 °C were not critical for *S.aureus* sterilization. Wang B et al. [21] found that PAW combined with mild heating (40–60 °C for 4 min) exhibited enhanced antibacterial activity against *L. monocytogenes* and *S. typhimurium*. Okyere A et al. [22] found that increasing the temperature of PAW improves the hydration properties of starch and gelatinization temperatures.

Clearly, the stability or reactivity of PAW is strongly dependent on the storage temperature and the temperature of pathogens to be treated by PAW. An increase in the temperature increases the reaction rate of RONS in PAW, thus affecting the inactivation process of pathogens in PAW. The PAW reactivity can be also dependent on the PAW temperature during the PAW production. The gas-phase RONS from the plasma will dissolve into water or react with water to generate PAW. Both Henry's law constant of the gas-phase RONS and the rate constant of chemical reactions in PAW are significantly affected by PAW temperature. The physical and chemical properties of PAW will be analyzed as a function of PAW temperature. Due to the low cost of gaseous materials, the method of air PAW has potential application prospects. Currently, complete inactivation *E. coli* of 10^4—10^6 CFU/mL by air PAW usually takes minutes of time [23–25]. However, the effect of PAW temperature during generation on their reactivity is not entirely understood. In this study, the PAW was prepared by using atmospheric pressure air DBD, and the biological and chemical reactivities of PAW will be evaluated by varying the temperature of treated water from 3 to 90 °C. By controlling the PAW temperature during generation, complete inactivation of *E. coli* (~ 10^4 CFU/mL) can be achieved in the order of seconds. The factors affecting the biological and chemical reactivities of PAW will be clarified in this study.

Material and Methods

Experimental Setup for Generating PAW

The plasma treatment system for generating PAW is schematically illustrated in Fig. 1. The system mainly consists of a dielectric barrier discharge reactor, a bubbling device, and an A.C. power supply. The DBD reactor includes a copper rod with its diameter of 54 mm, a quartz tube (inside diameter: 54 mm and outside diameter: 58 mm), and a stainless-steel tube with its inside diameter of 60 mm. The water-cooled stainless-steel tube acts as the ground electrode. The copper rad acts as the high-voltage electrode embedded in the quartz tube with its length of 750 mm. The compressed air ($H_2O \leq 3$ ppm) or O_2 (purity: 99.99%, $H_2O \leq 3$ ppm) flows through the plasma device at a flow rate of 10 standard liter per minute (SLM). The DBD is driven by the sine-wave voltage at a frequency of 10 kHz. The peak-to-peak voltage (V_{PP}) can be set within the range of 0 to 12 kV, leading to an increase in the discharge power (P) from 0 to 350 W, as measured by Lissajous figure [26]. The Lissajous figure is obtained by measuring the charges across the capacitor (2.2 μF) in series

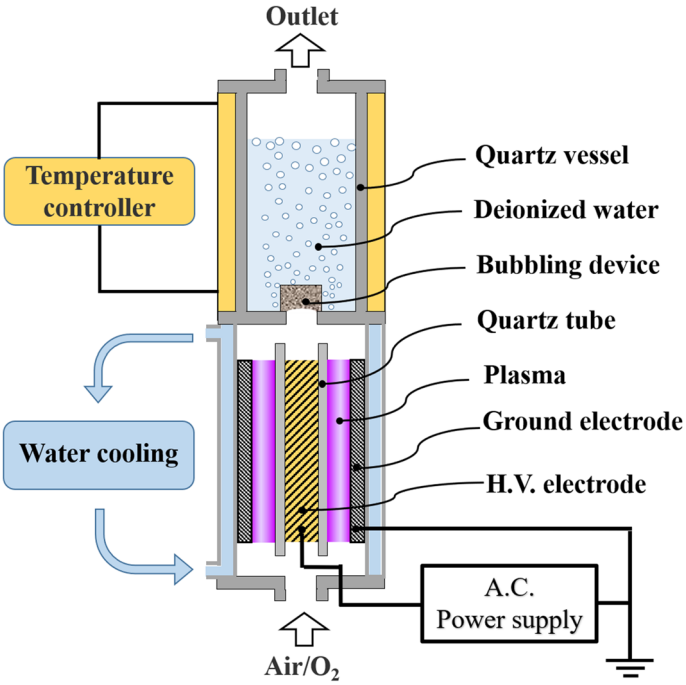

Fig. 1 The plasma treatment system for generating air or O_2 PAW

to ground electrode and the applied voltage across the plasma device. The air or O_2 DBD is produced in the gas spacing of 1.0 mm, and the DBD plasma is 0.14 L in volume. The exhaust gas containing O_3 or NO_X flows into the bubbling device to generate the bubbles in the sink. The bubbling device is made up of porous ceramics. The diameter of these bubbles in water is typically in the range of 1 to 3 mm, and their retention time is 0.2 s.

Before the discharge, the air or O_2 feeds through the DBD reactor for 45 min at a flow rate of 10 SLM. The temperature of 600 mL deionized (DI) water in the sink is controlled by the water bath outside the sink, which is typically 3 °C, 7.5 °C, 15 °C, 30 °C, 45 °C, 60 °C, 75 °C or 90 °C. The gas-phase RONS in the bubbles dissolve into DI water and react with each other, leading to the formation of air PAW or O_2 PAW. The plasma treatment time (t) varies from 0 to 320 s at a given P. To generate the consistent O_3 concentration of PAW, the air and O_2 plasma treatments were performed at P = 300 W and 270 W, respectively.

E. coli Sample Preparation and Treatment

The biological reactivity of PAW was evaluated by measuring the inactivation efficiency of *E. coli*. The *E. coli* was cultured in a lysogeny broth (LB) growth medium, and the initial bacterial concentration was ~ 10^7 CFU/mL. Four experiments were designed to evaluate the dependence of *E. coli* inactivation on the temperature (T) of DI water treated by the air or O_2 plasma.

2.2.1 *E. coli* inactivation by DI water at different temperature. The *E. coli* inactivation was also performed by changing DI water temperature from 3 to 90 °C. 600 µL of DI water with different temperatures was immediately added to the cuvette containing 20 µl of bacterial suspension. Then, the cuvette was immersed in the constant temperature (30 °C) bath for 5 min. After that, 300 µL of the mixed solutions was spread onto the LB agar medium. After overnight culture at 37 °C, colony counting was performed to determine the number of *E. Coli* survival in aqueous solution (CFU/mL). Data represent the mean and standard deviation of three independent biological replicates.
2.2.2 *E. coli* inactivation by air and O_2 PAW at different temperatures. After the air or O_2 plasma treatments at different temperatures, 600 µL of air or O_2 PAW was immediately added to the cuvette containing 20 µL of bacterial suspension. Then, the cuvette was immersed in the constant temperature (30 °C) bath for 5 min. After that, 300 µL of the mixed solution was spread onto the LB agar medium. After overnight culture at 37 °C, colony counting was performed to determine the number of *E. Coli* survival in aqueous solution (CFU/mL). Data represent the mean and standard deviation of three independent biological replicates.
2.2.3 *E. coli* inactivation by air and O_2 PAW at 30 °C. The air or O_2 PAW was first prepared at different temperatures. Then, 50 mL of PAW was immediately added to the cuvette containing the quartz beads with their diameter of 5 mm. The quartz beads were used to rapidly decrease or increase the PAW temperature to 30 °C. The quartz beads were previously heated or cooled, depending on PAW temperature. After that, 600 µL of 30 °C PAW was immediately added to the cuvette containing 20 µL of bacterial suspension, and the cuvette was immersed in the constant temperature (30 °C) bath for 5 min. 300 µL of the mixed solution was spread onto the LB agar medium. After overnight culture at 37 °C, colony counting was performed to determine the number of *E. Coli* survival in aqueous solution (CFU/mL). Data represent the mean and standard deviation of three independent biological replicates.
2.2.4 *E. coli* inactivation by O_2 PAW at the pH value of 2.8. To analyze the synergistic effect of aqueous O_3 and pH value on the *E. coli* inactivation, the O_2 plasma treatments of DI water were performed at the pH value of 2.8 to generate the acidic O_2 PAW. The H_2SO_4 solution was used to control the pH value of DI water. After the O_2 plasma treatments at different temperatures, 600 µL of PAW was immediately added to the cuvette containing 20 µL of bacterial suspension. Subsequently, the cuvette was immersed in the constant temperature (30 °C) bath for 5 min. Then, 300 µL of the mixed solution was spread onto the LB agar medium. After overnight culture at 37 °C, colony counting was performed to determine the number of *E. Coli* survival in aqueous solution (CFU/mL). Data represent the mean and standard deviation of three independent biological replicates.

NO_2^- and NO_3^- Concentrations of Air PAW

To measure the NO_3^- concentration, 1 mL of PAW was immediately added to 5 mL nickel sulfamate solution (purity > 98%, 50 g/L) after plasma treatment. Then, 3 mL of the mixed solution was measured by using UV/VIS-spectrophotometer (UV-1900, Shimadzu, Japan) at 219 nm. To measure the NO_2^- concentration, 60 µL of sulphanilamide solution (purity > 98%, 10 g/L) as the diazotizing reagent was immediately added to 3 mL of air PAW after the air plasma treatment. Then, the mixed solution was incubated at room temperature for 2 min. Subsequently, 60 µL of N-(1-Naphthyl)-ethylenediamine hydrochloride

(purity > 98%, 1 g/L) as the coupling reagent was added into the mixed solution. After reaction for 20 min at room temperature, the NO_2^- concentration was measured by using the UV-spectrophotometer at 540 nm [27].

O_3 Concentration of Air and O_2 PAWs

The concentration of O_3 in air and O_2 PAWs was determined by the iodometric titration method [28]. 100 ml of PAW was immediately added to 20 mL KI solution (purity > 98%, 200 g/L). Then the mixed solution was acidified with 5 ml H_2SO_4 solution (3 mol/L) immediately. After 5 min, $Na_2S_2O_3$ solution (purity > 98%, 0.05 mol/L) was used to titrate the mixed solution until it was pale yellow. After that, 1 mL starch solution (5 g/L) was added. The titrate was continued until it was colorless. The O_3 concentration was measured by calculating the total amount of sodium thiosulfate titration solution used.

H_2O_2 Concentration of Air PAW

For the H_2O_2 concentration measurements, 2 mL $TiSO_4$ (purity > 98%, 50 g/L) solution was immediately transferred to 2 mL air PAW after the air plasma treatment. Then, 4 mL H_2SO_4 solution was added to the mixed solution. After that, 3 mL solution was measured by using UV/VIS-spectrophotometer (UV-1900, Shimadzu, Japan) at 407 nm [29].

Conductivity and pH Value of Air and O_2 PAW

Both the pH value and conductivity of PAW were measured by a pH and conductivity analyzer (SI Analytics Co., model Lab-850, Germany).

Chemical Reactivity of Air and O_2 PAW

The chemical reactivity of air and O_2 PAWs is measured by using the chemical probe of terephthalic acid (TA). Terephthalic acid (TA) can be oxidized into 2-hydroxyterephthalic acid (HTA) by the activated oxygen in PAW, and HTA can be identified by fluorescence measurement [30, 31]. When the HTA solution is irradiated by UV light ($\lambda = 310$ nm), HTA molecules emit light at $\lambda = 425$ nm. The aqueous solution of TA (MΛCKLIN, purity > 98%) was prepared by dissolving TA in NaOH solution. The initial concentrations of TA and NaOH were 2 and 5 mM, respectively. 2 mL of TA solution was immediately added to 1 mL of PAW. The fluorescence measurements were performed by using a fluorescence spectrometer (Cary Eclipse 2018A43C). To quantify the concentration of HTA generated in the mixed solution, a calibration curve was obtained by using the standard HTA solution (MΛCKLIN, purity > 99%).

Results

The Effect of DI Water Temperature on E. coli Inactivation

The *E. coli* inactivation has been performed by using the DI water at different temperatures. The *E. coli* survival is almost independent on the DI water temperature varying from

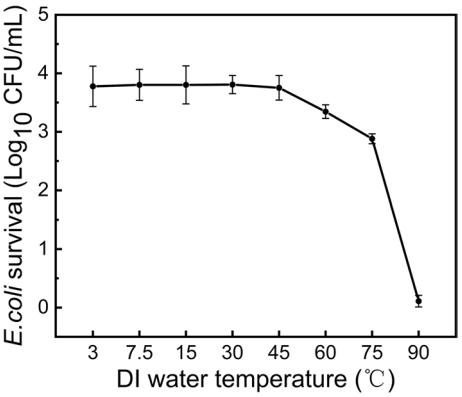

Fig. 2 The *E. coli* survival. *E. coli* were inactivated by using DI water at different temperatures

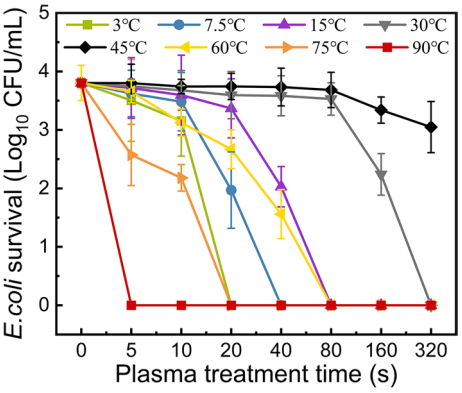

Fig. 3 *E. coli* inactivation by the air PAW prepared at different temperatures

3 to 45 °C (Fig. 2). However, the number of *E. coli* survival greatly decreases when the DI water temperature is higher than 45 °C. The survival rates of *E. coli* at 60 °C, 75 °C, and 90 °C are 37%, 13%, and 0.1%, respectively.

E. coli Inactivation by Air PAW

Figure 3 shows the *E. coli* inactivation by the air PAW prepared at different temperatures. The number of *E. coli* survival is strongly dependent on the plasma treatment time (t) varying from 0 to 320 s. At the temperature (T) of 3 °C, the *E. coli* is completely inactivated at $t \geq 20$ s. The times required for the complete inactivation of *E. coli* are 40 s at T = 7.5 °C, 80 s at T = 15 °C, and 320 s at T = 30 °C. At the T = 45 °C, the number of *E. coli* survival slowly decreases from 3.8 Log CFU/mL to 3.1 Log CFU/mL when t varies from 0 to 320 s. The biological reactivity of air PAW is greatly decreased when T increases from 3 to 45 °C. Compared to the other remote plasma treatment methods [1, 32], our bubbling device is effective for rapidly increasing the biological reactivity of PAW. Plenty of small bubbles are formed in the water, which contributes to an increase in the gas–liquid interface and the diffusion of gas-phase RONS into the water.

The times for the complete *E. coli* inactivation at T = 60 °C, T = 75 °C, and T = 90 °C are 80 s, 20 s, and 5 s, respectively (Fig. 3). Clearly, the biological reactivity of PAW is significantly increased when the PAW temperature increases from 45 to 90 °C. An increase

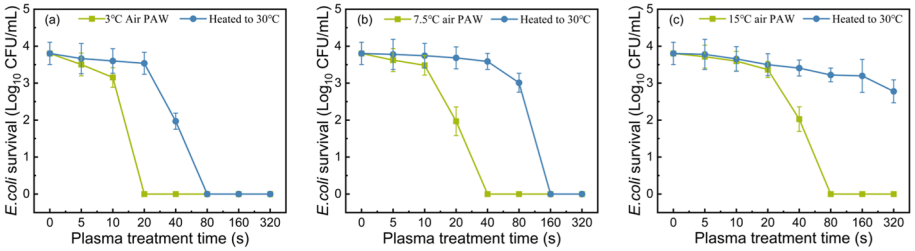

Fig. 4 The *E. coli* inactivation by low-temperature (≤ 15 °C) air PAW. The air PAW was prepared at the temperature of **a** 3 °C, **b** 7.5 °C, and **c** 15 °C. The low-temperature PAWs were used for the direct *E. coli* inactivation or for the *E. coli* inactivation after being heated to 30 °C

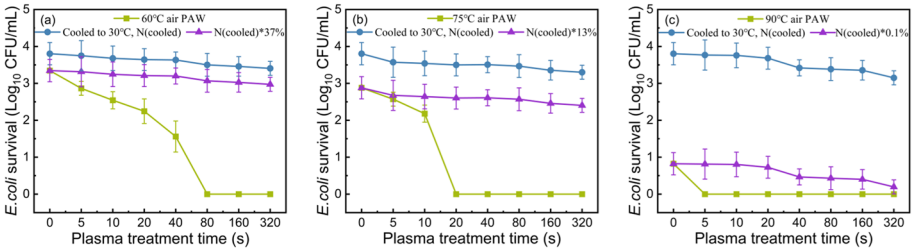

Fig. 5 The *E. coli* inactivation by 60–90 °C air PAW. The 60–90 °C air PAWs were used for the direct *E. coli* inactivation or for the *E. coli* inactivation after being cooled to 30 °C. The *E. coli* survival (N(T)) due to the combined effect of heat and RONS can be estimated from $N(T) = N(cooled) \times \eta(T)$, where N(cooled) is the *E. coli* survival due to the inactivation by the PAW cooled to 30 °C. η(T) is the survival rate of *E. coli* due to the DI water heated to T

in the biological reactivity can be closely related to an increase in the temperature of PAW. The study by Zhang et al. [19] indicates that the synergistic effect of PAW and mild heat can cause significant increases in membrane permeability, resulting in the leakage of intracellular components, such as nucleic acids and proteins. This effect could also increase the intracellular levels of reactive oxygen species. Decreasing PAW temperature from 45 to 3 °C is very helpful for increasing the biological reactivity of air PAW. After the low-temperature (≤ 15 °C) PAW is heated to 30 °C, the PAW reactivity is greatly decreased, as shown in Fig. 4. This suggests that increasing the temperature leads to a decrease in the stability of activated oxygen or their release from PAW.

The previous study has indicated that the sequential combination of washing with PAW followed by mild heating at 60 °C greatly decreases the counts of *Listeria monocytogenes* and *Staphylococcus aureus* [17]. Our study shows that the air PAW prepared at the temperature of ≥ 60 °C is very effective for the *E. coli* inactivation. Figure 5 shows that the biological reactivity of air PAW prepared at T = 60 – 90 °C is greatly reduced after being cooled to 30 °C. After being cooled to 30 °C, the biological reactivity of air PAW slightly increases with an increase in t, which is almost independent on T varying from 60 to 90 °C. This indicates that the concentration of RONS in PAW is greatly decreased at a relatively high PAW temperature. Increasing T decreases both the solubility and stability of RONS in PAW. The number of *E. coli* survival (N(T)) due to the combined effect of heat and RONS can be estimated as

$$N(T) = N(\text{cooled}) \times \eta(T)$$

where N(cooled) is the number of *E. coli* survival due to the inactivation by the PAW cooled to 30 °C. η(T) is the survival rate of *E. coli* due to the DI water heated to T. N(T) as a function of t is plotted in Fig. 5. The number of *E. coli* survivals after 60 – 90 °C PAW treatment is much lower than N(T), which confirms the synergistic effect of PAW and mild heat on the *E. coli* inactivation.

Physicochemical Properties of Air PAW

Both the pH value and conductivity of air PAW are strongly dependent on the plasma treatment time, t, as shown in Fig. 6. When t varies from 0 to 320 s, the pH value of PAW significantly decreases, accompanied by an increase in its conductivity. The PAW pH values of 2.4 – 3.2 are consistent with the ones reported previously [10, 17]. To identify the species in the plasma, Optical emission spectrum (OES) and Fourier-transform infrared spectrometer (FTIR) measurements has been conducted. Consistent with previous research [32–34], the emission data reveal that the species generated in the air discharge of the air DBD primarily include excited nitrogen molecules, nitrogen ions, oxygen atoms, and nitrogen atoms (figure S1). Further, FTIR spectrum indicates that the gas-phase species are mainly O_3 and N_2O (figure S2). A decrease in the pH value is primarily due to the dissolution of gas-phase NO, NO_2, N_2O_3, and N_2O_5 into DI water, and their subsequent reactions, leading to the formation of HNO_2 and HNO_3 in PAW [1, 2]. At a given t, decreasing T leads to a decrease in the pH value, accompanied by an increase in the conductivity (inserts in Fig. 6), indicating that the temperature can affect the Henry's law constants (H) of NO, NO_2, N_2O_3, and N_2O_5, which determines the highest achievable (saturated) concentration of these RONS in PAW. Decreasing T leads to an increase in the constant, thus an increase in the RONS concentration and a decrease in the pH value.

When t increases from 0 to 40 s, the NO_3^- concentration of air PAW slowly increases, then turns to significantly increase with t (Fig. 7a). However, the NO_2^- concentration rapidly increases when t varies from 0 to 40 s (Fig. 7b). The NO_2^- concentration remains almost unchanged when t is higher than 40 s. HNO_2 and HNO_3 can be generated due to the reactions of NO, NO_2, N_2O_3, and N_2O_5 with water, as shown below [1, 2, 35, 36].

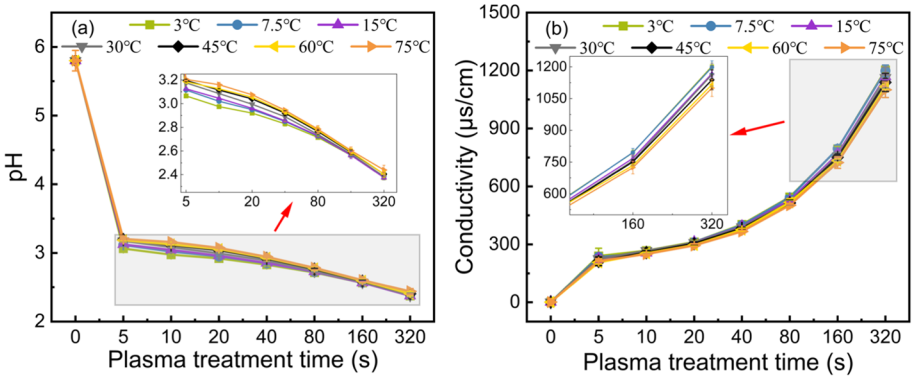

Fig. 6 The pH value (**a**) and conductivity (**b**) of air PAW as a function of the plasma treatment time. The air PAWs were prepared at different temperatures

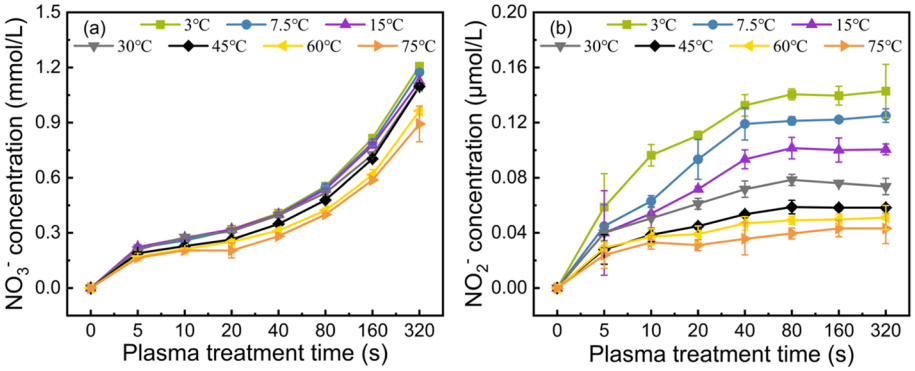

Fig. 7 The NO_3^- (**a**) and NO_2^- (**b**) concentrations of air PAW as a function of the plasma treatment time. The air PAWs were prepared at different temperatures

$$NO + NO_2 + H_2O \rightarrow 2NO_2^- + 2H^+ \quad (2)$$

$$N_2O_3 + H_2O \rightarrow HNO_2 + HNO_2 \quad (3)$$

$$NO_2 + NO_2 + H_2O \rightarrow NO_2^- + NO_3^- + 2H^+ \quad (4)$$

$$N_2O_5 + H_2O \rightarrow 2HOONO \rightarrow 2NO_3^- + 2H^+ \quad (5)$$

In PAW, NO_3^- is very stable, however, NO_2^- is very unstable. NO_2^- can be oxidized to NO_3^-, as shown below.

$$3NO_2^- + 3H^+ \rightarrow 2NO^- + NO_3^- + 3H^+ \quad (6)$$

$$NO_2^- + O_3 \rightarrow NO_3^- + O_2 \quad (7)$$

$$NO_2^- + H_2O_2 + H^+ \rightarrow HOONO + H_2O \rightarrow NO_3^- + H^+ + H_2O \quad (8)$$

Thus, NO_2^- concentration initially increases with t, then turns to remain unchanged due to the chemical reactions (R(6), R(7), and R(8)), leading to the formation of NO_3^-. This leads to a significant increase in the NO_3^- concentration at an increasing t. At a given t, both the NO_2^- and NO_3^- concentrations decrease with an increase in T, which shows that the solubility of gas-phase RONS is affected by the temperature.

The H_2O_2 concentration of PAW remains almost unchanged at ~ 7 μmol/L when t varies from 5 to 320 s (Fig. 8a). H_2O_2 can be generated by a combination of OH radicals from the homolysis of aqueous HOONO, as shown below [9].

$$HOONO \leftrightarrow OH + NO_2 \quad (9)$$

$$OH + OH \rightarrow H_2O_2 \quad (10)$$

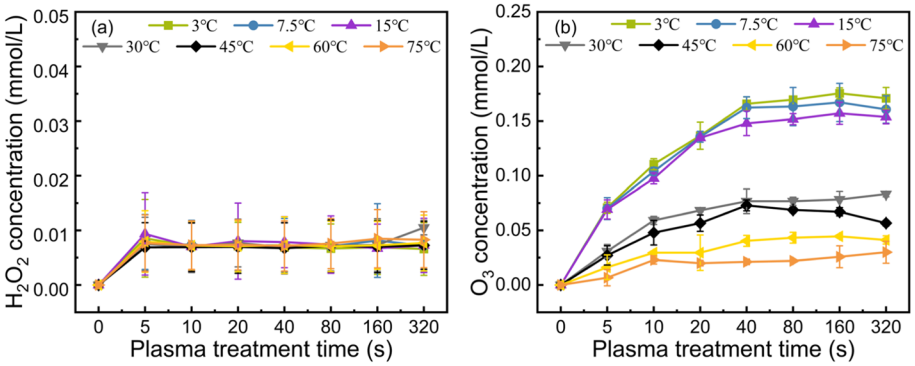

Fig. 8 The H_2O_2 (**a**) and O_3 (**b**) concentrations of air PAW as a function of the plasma treatment time. The air PAWs were prepared at different temperatures

The O_3 concentration of PAW initially increases with t, then remains almost unchanged when t is higher than 40 s (Fig. 8b). At a given t, the saturated concentration of O_3 in PAW decreases with an increase in T. This suggests that the solubility of O_3 in PAW is determined by the Henry's law constant, which greatly decreases with an increase in the temperature.

TA can be oxidized by the peroxide (activated oxygen [O]) in PAW, such as HOONO, H_2O_2, and O_3, which is used to evaluate the chemical reactivity of PAW [30, 31, 37, 38]. One TA can be converted into one HTA when one oxygen atom from the activated oxygen molecule is added to TA, as shown in Fig. 9. The oxidation rate is determined by the chemical activity of the peroxide or activated oxygen. Note that one OH radical in PAW will not lead to the complete oxidation of a TA molecule to a HTA molecule. However, the sequential reactions of two OH radicals with a TA molecule could lead to the complete oxidation of a TA molecule to a HTA molecule, accompanied by the formation of a H_2O molecule. The OH radicals will not play a crucial role in the oxidation process since their concentration is very low. Figure 10 shows that the HTA molecules are generated due to

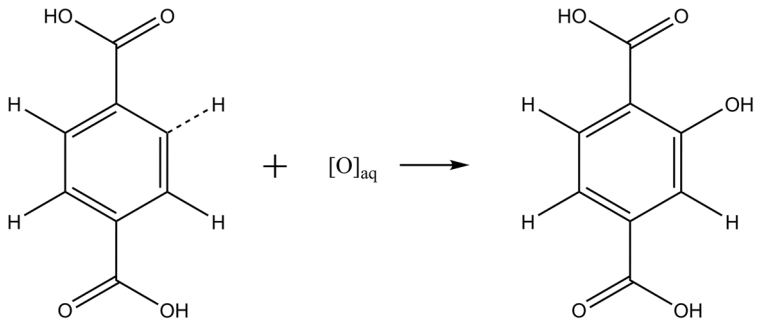

Fig. 9 The pathways for the oxidation of terephthalic acid (TA) into 2-hydroxyterephthalic acid (HTA) by the activated oxygen [O] in PAW. To generate one HTA molecule, one oxygen atom will be released from one activated oxygen [O] molecule during the oxidation process

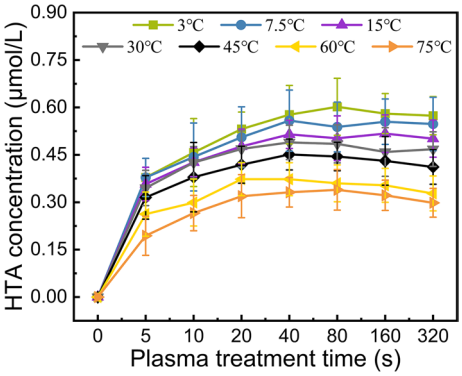

Fig. 10 The HTA concentration as a function of air plasma treatment time. The air PAWs were prepared at different temperatures. 2-hydroxyterephthalic acid (HTA) was generated due to the oxidation of terephthalic acid (TA) by the activated oxygen [O] in air PAW

the oxidation of TA by the activated oxygen in air PAW. The HTA concentration initially increases when t varies from 0 to 40 s. Then it remains unchanged when t is higher than 40 s. This indicates that the concentration of activated oxygen in air PAW remains constant when t is higher than 40 s. At a given t, decreasing T leads to a significant increase in the HTA concentration, indicating an increase in the chemical reactivity of PAW.

E. coli Inactivation by O_2 PAW

The O_2 PAW is prepared at different temperatures to evaluate the effect of O_3 on the *E. coli* inactivation. The O_3 concentration of O_2 PAW initially increases with t, then turns to remain unchanged with further increasing t (Fig. 11a), which is quite similar to the variation of O_3 concentration of air PAW with t. The pH value of O_2 PAW remains almost unchanged at 5.8. Decreasing T from 75 to 3 °C contributes to an obvious increase in the O_3 solubility. The O_2 PAW at the pH value of 5.8 is not very effective in the *E. coli* inactivation (Fig. 11b). Decreasing T from 30 to 3 °C or increasing T from 30 to 75 °C is helpful for increasing the biological reactivity of O_2 PAW.

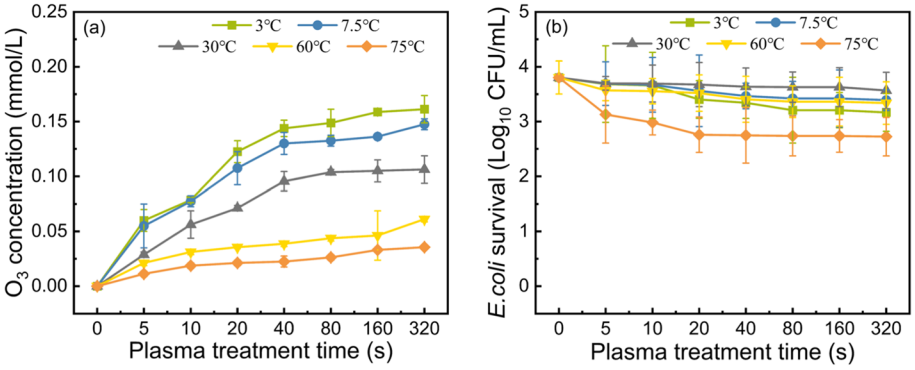

Fig. 11 **a** The O_3 concentration of O_2 PAW at the pH value of 5.8 as a function of plasma treatment time, and **b** the *E. coli* inactivation by the O_2 PAW at the pH value of 5.8. The O_2 PAWs were prepared at different temperatures

However, the O_2 PAW at the pH value of 2.8 is very effective in the *E. coli* inactivation (Fig. 12). Our study shows that the acidic solution at pH value of 2.8 has no obvious effect on the *E. coli* inactivation. The synergistic effect of O_3 and acidic solutions on the *E. coli* inactivation is still unclear. Decreasing T from 30 to 3 °C leads to an increase in the O_3 concentration, thus an improvement in the chemical reactivity of O_2 PAW. Increasing T from 30 to 75 °C leads to an increase in the biological reactivity of O_2 PAW, indicating the synergistic effect of O_3, temperature and a reduction in the pH value on the *E. coli* inactivation. However, the synergistic effect is not so obvious as the one from the air PAW. This indicates that other RONS, such as HOONO in the air PAW can also contribute to the synergistic effect on the *E. coli* inactivation.

Discussion

When the plasma-generated RONS flow through the bubbling system, some of them rapidly dissolve in water. The distribution equilibrium of a molecule in water and gas phases can be described by the dimensionless Henry's law constant $H(T) = C_{i,g}/C_{i,w}$, where $C_{i,g}$ and $C_{i,w}$ are the molar concentrations of molecules in the gas and water phases, respectively [39]. The temperature dependence of H(T) can be expressed as $\ln H = -A/RT + C$, where A is equal to $\Delta H^{\Theta}/R$, ΔH^{Θ} is the enthalpy change during the transfer of a molecule from the water phase to the gas phase, and C is temperature-independent constant. If the temperature dependence of ΔH^{Θ} is neglected, H(T) is significantly increased with an increase in T, which has been confirmed by experimental measurements [40, 41]. This indicates a decrease in the solubility of RONS in the water phase with an increase in the water temperature. It is previously reported that the concentration of O_3 in water decreases by ~ 40% when the water temperature increases from 20 °C to 40 °C [42]. The higher pH value at a relatively higher temperature can be attributed to a decrease in the solubility of RONS in air PAW.

It appears that the chemical reactivity of PAW is controlled by the activated oxygen in PAW. The RONS in PAW, including OH, HOONO, O_3 and H_2O_2 have a relatively high oxidation reduction potential, and they react with various functional groups in biomolecules,

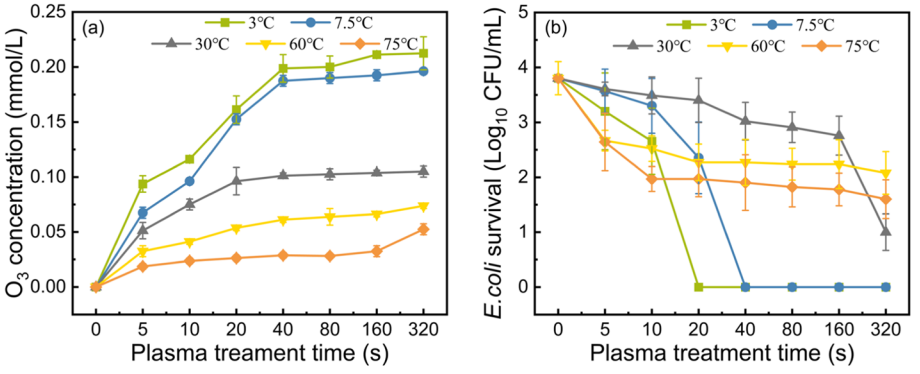

Fig. 12 **a** The O_3 concentration of O_2 PAW at the pH value of 2.8 as a function of plasma treatment time, and **b** the *E. coli* inactivation by the O_2 PAW at the pH value of 2.8. The O_2 PAWs were prepared at different temperatures

and damage the structures of DNA, proteins and lipids [31, 37, 43–46]. Increasing PAW temperature results in a decrease in the RONS concentration, thus a decrease in the chemical reactivity of PAW. The study by Moldgy et al. indicates that HOONO can be formed via the reaction of N_2O_5 with water (R5) [2]. However, HOONO is unstable, and they can decompose in acidic solutions via isomerization into HNO_3. This reaction rate is temperature–dependent, and the stability of HOONO in PAW decreases at a relatively high temperature. O_3 can be released from PAW due to an increase in the temperature, which decreases the chemical reactivity of PAW.

Our study indicates that the biological reactivity of PAW can be controlled by the synergistic effect of RONS, mild heat, and acidic solutions. The thermal stress can bring about many changes leading to the loss of viability, including enzyme inactivation, membrane damage, and nucleic acid breakdown. Heat can induce a breakage of hydrogen bonds and unfolding of the polypeptide chain, thus a collapse of the native protein structure [47]. Chick et al. [48] pointed to an analogy between disinfection by hot water and the coagulation of proteins as early as 1910. It is considered that moist heat kills bacterial cells by causing an intracellular coagulation of proteins. It has been proposed that an increase in the thermal sensitivity of *E. coli* is due to the low-temperature inactivation of an enzyme controlling an energy-yielding reaction [49]. The membrane damage has been caused by exposure to the high temperature [50]. The optical analysis of heated suspensions of *E. coli* indicates that the death of *E. coli* is due to the breakdown of intracellular RNA [51].

Reduction in the pH value of PAW results in a higher concentration of protonated acid, thus decreasing the polarity of the molecule and increasing diffusion of protonated acid across the membrane and into the cytoplasm. The reduction is proposed to affect the microbial activity by cytoplasmic acidification with subsequent uncoupling of energy production and regulation and by accumulation of the dissociated acid anion to toxic level [52]. The organic acid treatments of *E. coli* increase SYTOX orange permeation to ~ 30% of the maximum level [53]. The reduction in the pH value has been proposed to cause damage to the cellular membrane of *E. coli*, which contributes to an increase in permeabilization. When the intracellular pH value is decreased, the biological stress response system is induced, which can change the metabolic activity of cells. The leakage of intracellular constituents is generated by the increase in membrane permeability [54].

The synergistic combination of organic acids and ultraviolet (UV) has been previously reported to inactivate the bacteria cells [53, 55]. Analysis indicates that both damages to the bacterial cell membrane and intracellular esterase are closely related to the synergistic lethal effect. Higher water temperature (43 °C) is expected to increase the disinfection efficacy of chlorine by affecting the stability of the chemical disinfectant [56]. The enhanced efficacy of chlorine in the inactivation of bacterial cells could be a result of accelerated binding of chlorine to the cell surface. The synergistic inactivation of *S. cerevisiae* has been performed by the combined use of PAW and mild heat (40 – 50 °C) [18, 19]. The combined treatment of PAW and mild heat causes significant increases both in membrane permeability and the intracellular levels of reactive oxygen species, and the disruption of mitochondrial membrane potential. These RONS in air PAW including O_3, HOONO, H_2O_2 can also induce peroxidation of membrane lipids. This process can increase its permeability to RONS and protonated acids, thus cause the damage of RNA and proteins in cytoplasm. An obvious increase in the biological reactivity of low-temperature ($\leq$ 15 °C) air PAW is due to the synergistic effect of acidic solutions and a high concentration of RONS. The low biological reactivity of air PAW at 30–45 °C is attributed to the weak thermal stress and low RONS concentration of PAW. The biological reactivity of PAW at a higher water temperature (> 45 °C) can be controlled by the complex synergistic effects of RONS,

higher water temperature, and a reduction in the pH value. It appears that the death of *E. coli* induced by PAW is due, not only to the oxidation process by RONS, but also to the subtle changes in organized systems, which the bacteria cells are difficult to overcome.

Conclusion

In summary, we have prepared the air PAW at the water temperature of 3 – 90 °C, and evaluated the effect of temperature on the biological and chemical reactivities of air PAW. We have found that both biological and chemical reactivities of air PAW are strongly dependent on the PAW temperature. The chemical reactivity of PAW is significantly increased when the PAW temperature decreases from 90 to 3 °C. Decreasing the temperature from 30 to 3 °C or increasing the temperature from 45 to 90 °C significantly contributes to an increase in the biological reactivity of air PAW. This is consistent with previous research that sequential treatment of washing with PAW and mild heating at 60 °C can improve the microbiological quality of salted Chinese cabbage. Our analysis shows that an obvious increase in the biological reactivity of low-temperature ($\leq$15 °C) air PAW is due to the synergistic effect of acidic solutions and a high concentration of RONS. The high biological reactivity of air PAW at the temperature of $\geq$60 °C can be attributed to the synergistic effect of acidic solutions, heat and RONS, such as O_3 and HOONO.

Supplementary Information The online version contains supplementary material available at https://doi.org/10.1007/s11090-023-10379-y.

Authors' Contributions ZZ and DL performed the conceptualization and wrote the main manuscript text. HL performed the validation. ZQ performed the formal analysis. All authors reviewed the manuscript.

Funding This work was supported by Natural Science Foundation of China (12275042) and Natural Science Foundation of Liaoning Province of China (2023-BS-148).

Data Availability The data that support the findings of this study are available from the corresponding author upon reasonable request.

Declarations

Ethical Approval Not applicable.

Competing Interests I declare that the authors have no competing interests as defined by Springer, or other interests that might be perceived to influence the results and/or discussion reported in this paper.

References

1. Zhou R, Zhou R, Wang P, Xian Y, Mai-Prochnow A, Lu X, Cullen PJ, Ostrikov KK, Bazaka K (2020) Plasma-activated water: generation, origin of reactive species and biological applications. J Phys D Appl Phys 53:303001. https://doi.org/10.1088/1361-6463/ab81cf
2. Moldgy A, Nayak G, Aboubakr HA, Goyal SM, Bruggeman PJ (2020) Inactivation of virus and bacteria using cold atmospheric pressure air plasmas and the role of reactive nitrogen species. J Phys D Appl Phys 53:434004. https://doi.org/10.1088/1361-6463/aba066
3. Utsumi F, Kajiyama H, Nakamura K, Tanaka H, Mizuno M, Ishikawa K, Kondo H, Kano H, Hori M, Kikkawa F (2013) Effect of indirect nonequilibrium atmospheric pressure plasma on anti-proliferative activity against chronic chemo-resistant ovarian cancer cells in vitro and in vivo. PLoS One. 8:e81576. https://doi.org/10.1371/journal.pone.0081576

4. Ma R, Wang G, Tian Y, Wang K, Zhang J, Fang J (2015) Non-thermal plasma-activated water inactivation of food-borne pathogen on fresh produce. J Hazard Mater 300:643–651. https://doi.org/10.1016/j.jhazmat.2015.07.061
5. Zhou R, Zhou R, Zhang X, Zhuang J, Yang S, Bazaka K, Ostrikov K (2016) Effects of atmospheric-pressure N2, He, air, and O2 microplasmas on mung bean seed germination and seedling growth. Sci Rep-Uk. https://doi.org/10.1038/srep32603
6. Guo L, Yao Z, Yang L, Zhang H, Qi Y, Gou L, Xi W, Liu D, Zhang L, Cheng Y, Wang X, Rong M, Chen H, Kong MG (2021) Plasma-activated water: an alternative disinfectant for S protein inactivation to prevent SARS-CoV-2 infection. Chem Eng J. 421:127742. https://doi.org/10.1016/j.cej.2020.127742
7. Wang S, Xu D, Qi M, Li B, Peng S, Li Q, Zhang H, Liu D (2021) Plasma-activated water promotes wound healing by regulating inflammatory responses. Biophysica 1:297–310. https://doi.org/10.3390/biophysica1030022
8. Lamichhane P, Veerana M, Lim JS, Mumtaz S, Shrestha B, Kaushik NK, Park G, Choi EH (2021) Low-temperature plasma-assisted nitrogen fixation for corn plant growth and development. Int J Mol Sci 22:5360. https://doi.org/10.3390/ijms22105360
9. Goldstein S, Lind J, Merényi G (2005) Chemistry of peroxynitrites as compared to peroxynitrates. Chem Rev 105:2457–2470. https://doi.org/10.1021/cr0307087
10. Tsoukou E, Bourke P, Boehm D (2020) Temperature stability and effectiveness of plasma-activated liquids over an 18 months period. Water-Sui 12:3021. https://doi.org/10.3390/w12113021
11. Arda G, Hsu C (2023) Preservation of reactive species in frozen plasma-activated water and enhancement of its bactericidal activity through pH adjustment. Plasma Chem Plasma Process 43:599–618. https://doi.org/10.1088/1361-6463/ac286a
12. Chen J, Wang Z, Sun J, Zhou R, Guo L, Zhang H, Liu D, Rong M, Ostrikov KK (2023) Plasma-activated hydrogels for microbial disinfection. Adv Sci. https://doi.org/10.1002/advs.202207407
13. Shen J, Tian Y, Li Y, Ma R, Zhang Q, Zhang J, Fang J (2016) Bactericidal Effects against S. aureus and Physicochemical Properties of Plasma Activated Water stored at different temperatures. Sci Rep 6:28505. https://doi.org/10.1038/srep28505
14. Subramanian P, Jain A, Shivapuji A, Sundaresan N, Dasappa S, Rao L (2020) Plasma-activated water from a dielectric barrier discharge plasma source for the selective treatment of cancer cells. Plasma Process Polym 17:1900260
15. Rathore V, Nema S (2021) Optimization of process parameters to generate plasma activated water and study of physicochemical properties of plasma activated solutions at optimum condition. J Appl Phys 129:084901. https://doi.org/10.1063/5.0033848
16. Pang B, Liu Z, Zhang H, Wang S, Gao Y, Xu D, Liu D, Kong M (2022) Investigation of the chemical characteristics and anticancer effect of plasma-activated water: The effect of liquid temperature. Plasma Process Polym 19:2100079. https://doi.org/10.1002/ppap.202100079
17. Choi EJ, Park HW, Kim SB, Ryu S, Lim J, Hong EJ, Byeon YS, Chun HH (2019) Sequential application of plasma-activated water and mild heating improves microbiological quality of ready-to-use shredded salted kimchi cabbage (Brassica pekinensis L.). Food Control 98:501–509. https://doi.org/10.1016/j.foodcont.2018.12.007
18. Xiang Q, Zhang R, Fan L, Ma Y, Wu D, Li K, Bai Y (2020) Microbial inactivation and quality of grapes treated by plasma-activated water combined with mild heat. LWT. 126:109336. https://doi.org/10.1016/j.lwt.2020.109336
19. Zhang R, Ma Y, Wu DI, Fan L, Bai Y, Xiang Q (2020) Synergistic inactivation mechanism of combined plasma-activated water and mild heat against saccharomyces cerevisiae. J Food Protect 83:1307–1314. https://doi.org/10.4315/JFP-20-065
20. Tian Y, Ma R, Zhang Q, Feng H, Liang Y, Zhang J, Fang J (2015) Assessment of the physicochemical properties and biological effects of water activated by non-thermal plasma above and beneath the water surface. Plasma Process Polym 12:439–449. https://doi.org/10.1002/ppap.201400082
21. Wang B, Wang W, Xiang Q, Bai Y (2023) Effects of heating on the antibacterial efficacy and physicochemical properties of plasma-activated water. Qual Assur Saf Crop Foods 15:100–108
22. Okyere A, Boakye P, Bertoft E, Annor G (2022) Temperature of plasma-activated water and its effect on the thermal and chemical surface properties of cereal and tuber starches. Curr Res Food Sci 5:1668–1675. https://doi.org/10.1016/j.crfs.2022.09.020
23. Man C, Zhang C, Fang H, Zhou R, Huang B, Xu Y, Zhang X, Shao T (2022) Nanosecond-pulsed microbubble plasma reactor for plasma-activated water generation and bacterial inactivation. Plasma Process Polym. 19:e2200004. https://doi.org/10.1002/ppap.202200004
24. Rothwell J, Alam D, Carter D, Soltani B, Mcconchie R, Zhou R, Cullen P, Mai-Prochnow A (2022) The antimicrobial efficacy of plasma-activated water against Listeria and E. coli is modulated by

reactor design and water composition. J Appl Microbiol 132:2490–2500. https://doi.org/10.1111/jam.15429
25. Wang Q, Salvi D (2021) Evaluation of plasma-activated water (PAW) as a novel disinfectant: Effectiveness on Escherichia coli and Listeria innocua, physicochemical properties, and storage stability. LWT 149:111847. https://doi.org/10.1016/j.lwt.2021.111847
26. Falkenstein Z, Coogan JJ (1997) Microdischarge behaviour in the silent discharge of nitrogen - oxygen and water - air mixtures. J Phys D Appl Phys 30:817–825. https://doi.org/10.1088/0022-3727/30/5/015
27. Qi Z, Tian E, Song Y, Sosnin EA, Skakun VS, Li T, Xia Y, Zhao Y, Lin X, Liu D (2018) Inactivation of Shewanella putrefaciens by plasma activated water. Plasma Chem Plasma 38:1035–1050. https://doi.org/10.1007/s11090-018-9911-5
28. Chasanah U, Yulianto E, Zain AZ, Sasmita E, Restiwijaya M, Kinandana AW, Arianto F, Nur M (2019) Evaluation of titration method on determination of ozone concentration produced by dielectric barrier discharge plasma (DBDP) Technology. J Phys: Conf Ser 1153:12086. https://doi.org/10.1088/1742-6596/1153/1/012086
29. Marotta E, Ceriani E, Schiorlin M, Ceretta C, Paradisi C (2012) Comparison of the rates of phenol advanced oxidation in deionized and tap water within a dielectric barrier discharge reactor. Water Res 46:6239–6246. https://doi.org/10.1016/j.watres.2012.08.022
30. Kanazawa S, Furuki T, Nakaji T, Akamine S, Ichiki R (2013) Application of chemical dosimetry to hydroxyl radical measurement during underwater discharge. J Phys Conf Ser 418:12102–12107. https://doi.org/10.1088/1742-6596/418/1/012102
31. Liu X, Wang Z, Li J, Wang Y, Sun Y, Dou D, Liang X, Wu J, Wang L, Xu Y, Liu D (2022) Inactivation of E. coli, S. aureus, and Bacteriophages in biofilms by humidified air plasma. Int J Mol Sci. 23:4856. https://doi.org/10.3390/ijms23094856
32. Xi W, Wang W, Liu Z, Wang Z, Guo L, Wang X, Rong M, Liu D (2020) Mode transition of air surface micro-discharge and its effect on the water activation and antibacterial activity. Plasma Sources Sci T 29:95013. https://doi.org/10.1088/1361-6595/aba7ef
33. Zhou S, Su L, Shi T, Zheng T, Tong Y, Nie W, Che X, Zhao J (2019) Experimental study on the diffusive flame stabilization mechanism of plasma injector driven by AC dielectric barrier discharge. J Phys D Appl Phys 52:265202. https://doi.org/10.1088/1361-6463/ab15cd]
34. Shen J, Tian Y, Li Y, Ma R, Zhang Q, Zhang J, Fang J (2016) Bactericidal Effects against S. aureus and physicochemical properties of plasma activated water stored at different temperatures. Sci Rep. https://doi.org/10.1038/srep28505
35. Machala Z, Tarabova B, Hensel K, Spetlikova E, Sikurova L, Lukes P (2013) Formation of ROS and RNS in water electro-sprayed through transient spark discharge in air and their bactericidal effects. Plasma Process Polym 10:649–659. https://doi.org/10.1002/ppap.201200113
36. NDRL/NIST Solution Kinetics Database US. http://kinetics.nist.gov/solution/. Accessed 03 March 2022
37. Cataldo F (2006) Ozone degradation of biological macromolecules: Proteins, haemoglobin, RNA, and DNA. Ozone Sci Eng. 28:317–328. https://doi.org/10.1080/01919510600900290
38. Lukes P, Dolezalova E, Sisrova I, Clupek M (2014) Aqueous-phase chemistry and bactericidal effects from an air discharge plasma in contact with water: evidence for the formation of peroxynitrite through a pseudo-second-order post-discharge reaction of H_2O_2 and HNO_2. Plasma Sources Sci. https://doi.org/10.1088/0963-0252/23/1/015019
39. Görgényi M, Dewulf J, Langenhove HV (2002) Temperature dependence of Henry's law constant in an extended temperature range. Chemosphere (Oxford) 48:757–762. https://doi.org/10.1016/S0045-6535(02)00131-5
40. Nirmalakhandan N, Brennan RA, Speece RE (1997) Predicting Henry's Law constant and the effect of temperature on Henry's Law constant. Water Res 31:1471–1481. https://doi.org/10.1016/S0043-1354(96)00395-8
41. Dewulf J, Drijvers D, Langenhove HV (1995) Measurement of Henry's law constant as function of temperature and salinity for the low temperature range. Armos Environ 29:323–331. https://doi.org/10.1016/1352-2310(94)00256-K
42. Levanov AV, Isaikina OY, Lunin VV (2019) Thermodynamic and kinetic parameters of the solubility of ozone in water. Russ J Phys Chem A. 93:1230–1234. https://doi.org/10.1134/S0036024419070148
43. Wright A, Bubb WA, Hawkins CL, Davies MJ (2002) Singlet oxygen-mediated protein oxidation: evidence for the formation of reactive side chain peroxides on tyrosine residues. Photochem Photobiol 76:35–46. https://doi.org/10.1562/0031-8655(2002)076%3c0035:sompoe%3e2.0.co;2
44. Spanggord RJ, Yao CD, Mill T (2000) Oxidation of Aminodinitrotoluenes with ozone: Products and pathways. Environ Sci Technol 34:497–504. https://doi.org/10.1021/es990190h

45. Radil R, Beckman JS, Bush KM, Freeman BA (1991) Peroxynitrite oxidation of sulfhydryls: the cytotoxic potential of superoxide and nitric oxide. J Biol Chem 266:4244–4250. https://doi.org/10.1016/S0021-9258(20)64313-7
46. Uppu RM, Pryor WA (1994) The reactions of ozone with proteins and unsaturated fatty acids in reverse micelles. Chem Res Toxicol 7:47–55. https://doi.org/10.1021/tx00037a007
47. Allwood MC, Russell AD (1970) Mechanisms of thermal injury in nonsporulating bacteria. Adv Appl Microbiol 12:89–119. https://doi.org/10.1016/S0065-2164(08)70583-5
48. Chick H (1910) The process of disinfection by chemical agencies and hot water. J Hyg 10:238–286. https://doi.org/10.1017/S0022172400042959
49. Cousin D (1967) Thermosensitive mutants of Escherichia coli k12.2. studies on a lethal mutation controlling an energy yielding reaction. Ann Inst Pasteur 113:309–325
50. Russell AD, Harries D (1967) Some aspects of thermal injury in Escherichia coli. Appl Microbiol 15:407–410. https://doi.org/10.1128/am.15.2.407-410.1967
51. Califano L (1952) Libération d'acide nucléique par les cellules bactériennes sous l'action de la chaleur. Bull World Health Organ 6:19–34
52. Mani-López E, García HS, López-Malo A (2012) Organic acids as antimicrobials to control Salmonella in meat and poultry products. Food Res Int 45:713–721. https://doi.org/10.1016/j.foodres.2011.04.043
53. De Oliveira EF, Cossu A, Tikekar RV, Nitin N (2017) Enhanced antimicrobial activity based on a synergistic combination of sublethal levels of stresses induced by UVa light and organic acids. Appl Environ Microbiol 83:e00383-e417. https://doi.org/10.1128/AEM.00383-17
54. Hao J, Lei Y, Gan Z, Zhao W, Shi J, Jia C, Sun A (2021) Synergetic inactivation mechanism of protocatechuic acid and high hydrostatic pressure against escherichia coli O157:H7. Foods 10:3053. https://doi.org/10.3390/foods10123053
55. Jeong Y, Ha J (2019) Combined treatment of UV-A radiation and acetic acid to control foodborne pathogens on spinach and characterization of their synergistic bactericidal mechanisms. Food Control. 106:106698. https://doi.org/10.1016/j.foodcont.2019.06.024
56. Muraca P, Stout JE, Yu VL (1987) Comparative assessment of chlorine, heat, ozone, and UV light for killing Legionella pneumophila within a model plumbing system. Appl Environ Microbiol 53:447–453. https://doi.org/10.1128/aem.53.2.447-453.1987

Publisher's Note Springer Nature remains neutral with regard to jurisdictional claims in published maps and institutional affiliations.

Springer Nature or its licensor (e.g. a society or other partner) holds exclusive rights to this article under a publishing agreement with the author(s) or other rightsholder(s); author self-archiving of the accepted manuscript version of this article is solely governed by the terms of such publishing agreement and applicable law.